Hydrogen Bonds and H_3O^+ Formation at the Water Interface with Formic Acid Covered Anatase TiO_2

Bo Wen[1,2] and Annabella Selloni[1]

1 *Department of Chemistry, Princeton University, New Jersey 08544, USA*

2 *School of Physics and Electronics, Henan University, Kaifeng 475001, P. R. China.*

Abstract

Carboxylic acid-modified TiO_2 surfaces in aqueous environment are of widespread interest, yet atomic-scale understanding of their structure is limited. We here investigate formic acid (FA) on anatase TiO_2 (101) (A-101) in contact with water using density functional theory (DFT) and ab-initio molecular dynamics (AIMD). Isolated FA molecules adsorbed in a deprotonated bridging bidentate (BD) form on A-101 are found to remain stable at the interface with water, with the acid proton transferred to a surface oxygen to form a surface bridging hydroxyl ($O_{br}H$). With increasing FA coverage, adsorbed monolayers of only BD and successively of alternating monodentate (MD) and BD species give rise to a higher concentration of surface $O_{br}H$'s. Simulations of these adsorbed monolayers in water environment show that some protons are released from the surface $O_{br}H$'s to water resulting in a negatively charged surface with nearby solvated H_3O^+ ions. These results provide insight into the complex acid-base equilibrium between an oxide surface, adsorbates and water and can also help obtain a better understanding of the wetting properties of chemically modified TiO_2 surfaces.

Introduction

The combined interactions of carboxylic acids and water with TiO_2 surfaces are of critical importance in many fields and applications, from atmospheric chemistry and photocatalysis to solar cells, and biomedical devices[1-7]. For example, carboxylic acids are widely used to anchor dye

sensitizers and other functional molecules to TiO_2[8,9], but the competition of water for binding to the oxide surface can limit the long-term stability of the functional attachment and thus the lifetime of various devices. In atmospheric chemistry, the uptake and photo-oxidation of formic and acetic acid on TiO_2 dust particles are instead enhanced by the presence of co-adsorbed water[4,10]. These organic acids are also found to adsorb selectively on rutile TiO_2 (110) exposed to air and ambient water, where they form ordered monolayers of adsorbed formate/acetate species even though other volatile compounds are present in much higher concentrations[11].

The formation of such organic monolayers on TiO_2 has further implications. It could explain the UV induced hydrophilicity and self-cleaning properties of TiO_2 surfaces and could also be relevant in photocatalysis[11]. However, self-cleaning windows and photocatalysis are typically based on anatase rather than on the rutile form of TiO_2, and these two phases are known to exhibit distinct surface chemistries[1,12-14]. Although several studies involving water and carboxylic acids on anatase surfaces are available, unclear aspects still exist. For example, some experiments found carboxylic acids to adsorb more strongly than water and to displace it from the surface[6,15]. In contrast, other studies reported that adsorbed formate/acetate species are solvated by co-adsorbed water molecules and their coordination to the surface changes from bridging bidentate to monodentate[10,16] Further understanding of the interactions of carboxylic acids and water with anatase can clarify these issues and could also help to improve their control in various applications.

To contribute to this understanding, we focus on the adsorption of formic acid (FA) at the aqueous interface with anatase TiO_2 (101) (A-101), the most abundant surface of anatase. As the simplest carboxylic acid, FA is often used as a prototypical molecule for probing the reactivity of TiO_2 surfaces[12,17-19]. In particular, recent surface science experiments under UHV conditions have shown that the most stable FA adsorption state on A-101 is a deprotonated bidentate (BD) configuration at low and intermediate coverages, while a (3×1) periodic arrangement of alternating monodentate (MD) and BD species becomes favorable at saturation coverage[18]. Starting from these structures, we have studied their behavior in water environment using ab-initio molecular dynamics (AIMD) based on the strongly constrained and appropriately normed (SCAN) density functional[20], known to well describe H-bonds and van der Waals (vdW) interactions in the intermediate range scale[21,22] (see details in Supporting Information, SI). Our results show that adsorbed formate species on A-101 are stable upon solvation in water, within the typical time scale of AIMD simulations. However, some of the acid protons are released from the surface to the

surrounding water environment in the case of high coverage adsorption, leading to an electrical double layer that can significantly affect the interface reactivity[23].

Let us start by considering the adsorption structures of an isolated FA on A-101 in vacuum (Figure 1). The A-101 surface exposes alternating rows of undercoordinated 5-fold Ti (Ti_{5c}) and 2-fold bridging oxygen (O_{br}) atoms along the [010] direction. FA can bind to the Ti_{5c} sites in molecular monodentate (MD), deprotonated MD and deprotonated bidentate (BD) forms. In the deprotonated structures, the acid proton is transferred from FA to a nearby O_{br} resulting in a bridging OH group ($O_{br}H$); this forms a short H-bond with the formate in the case of the MD configuration[24]. The adsorption energies calculated with SCAN, also given in Figure 1, indicate that the deprotonated BD structure is most stable, in agreement with experiments[18]. For comparison, we also carried out calculations using the standard semi-local functional of Perdew, Burke and Ernzerhof (PBE)[25], and found the molecular MD structure to be most favorable (Table S1, SI), in agreement with earlier studies.[7] The difference between PBE and SCAN predictions can be attributed to the partial inclusion of vdW interactions in the latter functional[21,22,26]; PBE calculations including vdW corrections predict indeed the BD configuration to be most stable.[19]

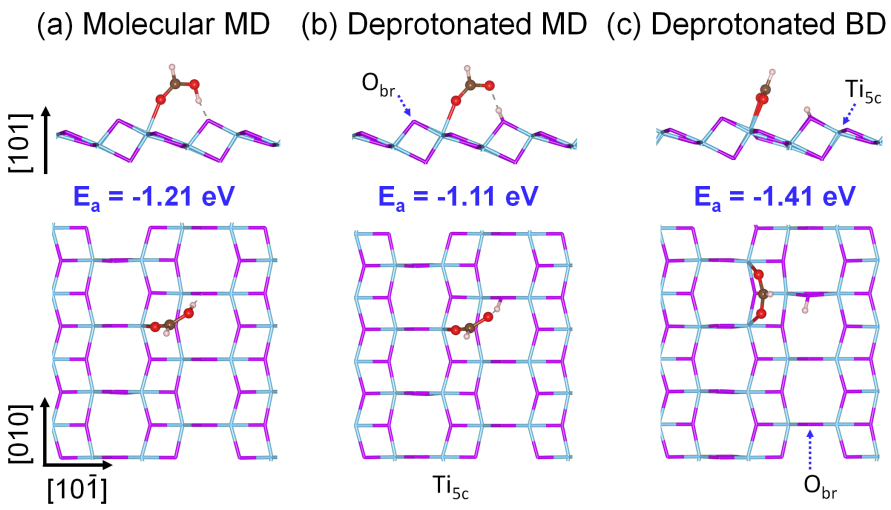

Figure 1 – Computed (SCAN) adsorption structures and energies (E_a) for FA (0.125 ML) on defect-free A-101 in vacuum: (a) Molecular monodentate (MD), (b) deprotonated MD and (c) deprotonated bidentate (BD) with nearby $O_{br}H$ group. For better visualization, side (upper panels) and top views (lower panels) of only the surface layer are shown; the substrate and FA are represented with stick and ball-and-stick models, respectively. Blue, purple, red, brown, and white stick/balls stand for Ti, O of TiO_2, O of FA, C and H, respectively.

We investigated low coverage FA adsorption under wet conditions using a four layers A-101 (4×1) slab with one adsorbed BD formate and one accompanying $O_{br}H$ on each surface while the water environment was represented by 75 molecules at the experimental density of 1g/cm^3. Figure 2a shows a snapshot and the average water density profile of this interface (denoted **I1** in the following) as given by our AIMD simulation. The density is characterized by a first sharp peak at ~ 2.2 Å above each TiO_2 surface, corresponding to a densely packed layer of intact H_2O molecules adsorbed at surface Ti_{5c} sites, followed by a smaller and broader peak mostly composed of water molecules forming H-bonds with the surface O_{br} sites[26]. At larger distance from the surface, a third weak peak is also present, in agreement with the interfacial water structure on adsorbate-free A-101 reported previously[26-29]. Further details on the water structure are given in the Supporting Information, together with the results of analogous PBE simulations (Figures S1 and S2).

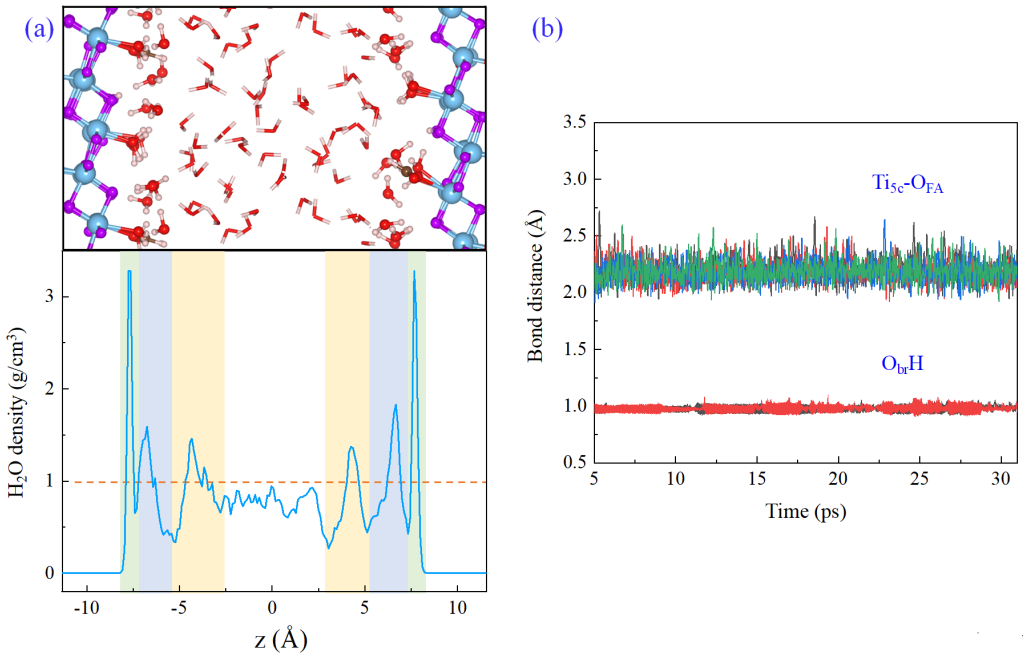

Figure 2 – Low coverage formic acid adsorption on A-101 in contact with water (interface **I1**). (a) Snapshot (top) and average water density profile (bottom); the different shades highlight the first (green), second (blue) and third (yellow) interfacial water layers; the horizontal dashed line (in orange) indicates the density of bulk liquid water. (b) Time evolution of the four Ti_{5c}-O_{FA} and two $O_{br}H$ bond lengths in (a), from SCAN-based AIMD trajectory at 330 K. Results after 5 *ps* equilibration are shown.

To characterize the FA adsorption structure at the aqueous interface, we monitored the time evolution of the Ti_{5c}-O_{FA} bond lengths of the two adsorbed BD species (total 4 bonds) along the

AIMD trajectory (Figure 2b). The resulting average bond lengths are 2.19 - 2.20 Å with root mean square deviations (RMSD) of 0.092 - 0.104 Å, to be compared to Ti_{5c}-O_{FA} bond lengths of ~ 2.06 Å in vacuum (Table S2). The limited range of the RMSD indicates that the adsorbed BD species remain stable at the interface with water, within the time scale of our simulation. However, the significant Ti_{5c}-O_{FA} bond elongation for the solvated system relative to the bond length in vacuum implies a weakening of the FA binding to the surface, due to both H-bonding with neighboring water molecules and overall solvent polarization. The latter effect was estimated using a periodic continuum solvation model (PCSM)[30] (see SI) and found to cause a reduction of the FA binding energy from -1.41 to -1.07 eV for the vacuum-optimized structure. Considering that the Ti_{5c}-O_{FA} bond lengths are actually elongated (~ 2.19 Å) in the simulation, we obtain an estimated binding energy of -0.93 eV for the adsorbed FA in water, i.e., ~ 0.5 eV weaker than that in vacuum. For comparison, PBE-based simulations show the breaking of one Ti_{5c}-O_{FA} bond with transformation of a BD formate to the MD configuration (Figure S3), consistent with the greater stability of MD vs BD species in vacuum predicted by the PBE functional.

Turning next to high coverage adsorption, experimental studies of acetic and formic acid on A-101 under UHV conditions have revealed the formation of monolayers of BD (0.5ML) and mixed MD/BD (0.67 ML) species, with $O_{br}H$ hydroxyls resulting from the dissociated acid protons adsorbed at the bridging oxygen sites[18,31] (Figure S4). A snapshot of a monolayer of BD formates and accompanying $O_{br}H$'s in contact with water (interface **I2**) is shown in Figure 3a, together with the average water density profile from our AIMD simulation. Since the monolayer of BD formates leaves no available Ti_{5c} sites for water adsorption on the A-101 surface, the hydration layer of the clean A-TiO_2 surface is largely suppressed. The first peak of the water density profile (shaded in blue in Figure 3a) has now a height of 1.5-2 g/cm^3, which is similar to that of the second peak in the low coverage profile of Figure 2a. This also suggests that the first water layer above the monolayer of BD formates on A-101 may originate from water molecules hydrogen bonded with surface O_{br} and $O_{br}H$ groups. We will return to this feature in more detail in the following.

The time evolution of the Ti_{5c}-O_{FA} bond lengths at the **I2** interface is reported in Figure S5. Comparison of the average bond lengths, in the range 2.09 – 2.13 Å, with the bond distance of 2.075 Å for the adsorbed formate monolayer in vacuum (T= 0K) shows elongations much smaller than those found for isolated adsorbed species (compare Table S2 and Table S3). Moreover, while in vacuum the Ti_{5c}-O_{FA} bond lengths are slightly larger for the monolayer than for isolated

molecules, the reverse is true in water. This indicates that the solvent-induced destabilization of the molecule-surface binding is weaker in the case of the monolayer than for isolated adsorbed molecules, which we attribute to the weaker contribution of H-bonding with neighboring water molecules. Calculations using the PCSM[30] give a reduction of the monolayer adsorption energy from -1.39 to -0.96 eV/FA for the vacuum-optimized structure.

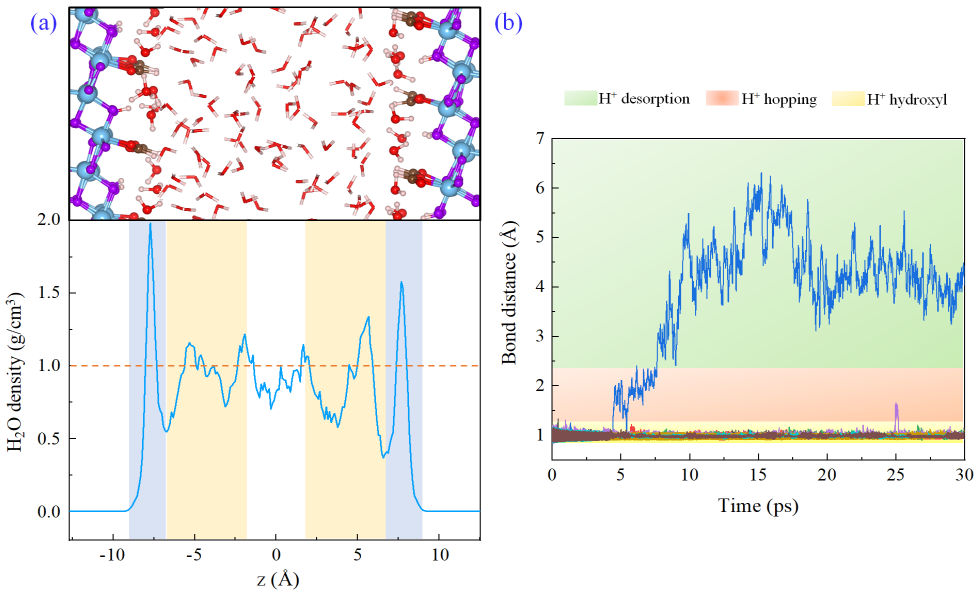

Figure 3 – Formic acid monolayer of BD species on A-101 in contact with water (interface **I2**). (a) Snapshot (top) and water density profile (bottom) from AIMD simulation; the presence of H_3O^+ closer to the left interface makes the water density profile asymmetric. (b) Time evolution of the O_{br}-H_{BD} bond distances; yellow, pink and green shades indicate distances corresponding to protons adsorbed at surface O_{br} sites ($O_{br}H$), protons hopping along surface O_{br} sites, and protons in H_3O^+ ions away from the surface, respectively.

Lastly, we examine the behavior of the acid protons at the aqueous **I2** interface. As shown by the time evolution of the $O_{br}H$ bond distances in Figure 3b, one of the $O_{br}H$ bond distances starts to become increasingly larger after a few ps of simulation time, indicating that a proton, initially adsorbed on a surface oxygen site, diffuses into water to form a H_3O^+ ion. We note that transient H_3O^+ species have been observed in previous simulations of the A-TiO_2-water interface or in the reaction of molecular species with water[29,32,33]. In the present study, however, the aqueous H_3O^+ has a long lifetime (on the time scale of our simulation) and is not confined to the immediate

vicinity of the interface, suggesting that the process of proton transfer to water is not driven by kinetics but rather by thermodynamics, i.e., by the enhanced acidity of the FA covered surface. To estimate the surface acidity, we calculated the energy required to detach one proton from the surface and bring it to the center of the solvation region using the PCSM[30] (see SI). We found that the energy cost to desorb a proton is ~ 0.7 eV lower for the FA-covered surface than for the water-covered one, implying that the surface pKa becomes strongly negative in the presence of the adsorbed FA monolayer[23,34]. This result also implies that the use of the deuteron (instead of the proton) mass in our simulations has no significant effect on the observed reactions.

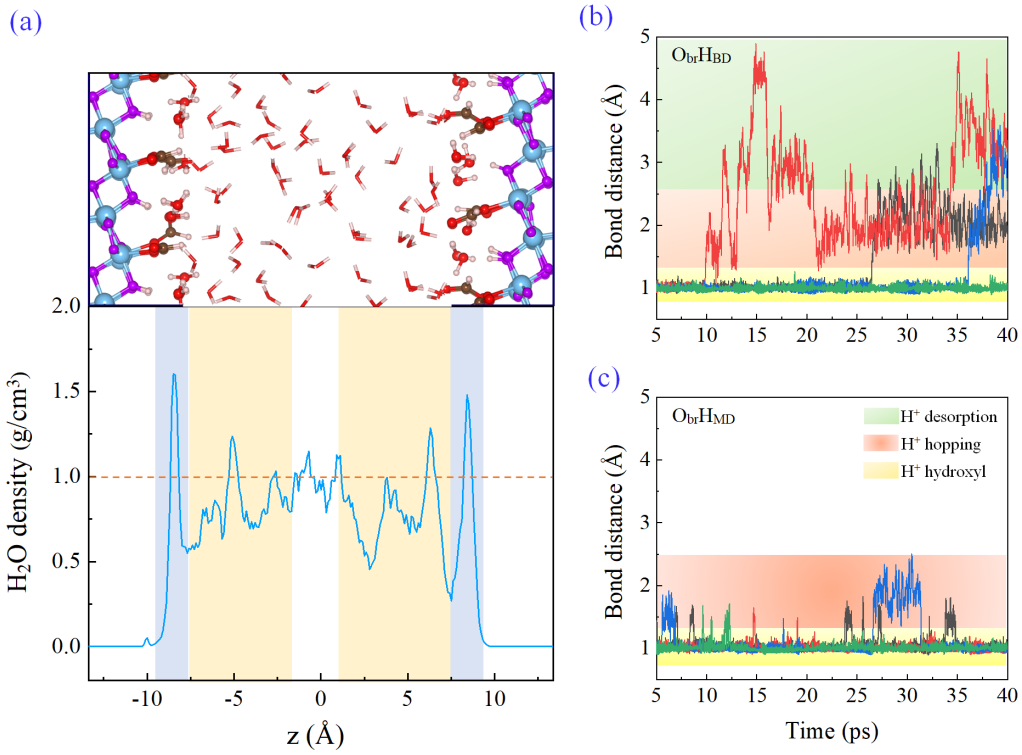

Figure 4 – Formic acid monolayer of mixed MD/BD species on A-101 in contact with water (interface **I3**). (a) Snapshot (top panel) and water density profile (lower panel) from AIMD simulation; the first peak of the water distribution is similar but less pronounced than the one at the **I2** interface; both MD and BD species are stable during the simulation (Figure S5). (b, c) Time evolution of O_{br}-H_{BD} (top) and O_{br}-H_{MD} (bottom) bond distances. Results after 5 *ps* equilibration are shown.

To confirm this hypothesis, we further investigated the water interface with an adsorbed monolayer of mixed MD/BD formates (interface **I3**; see Figures 4a and S5). Interestingly, analysis

of the time evolution of the $O_{br}H$ bond lengths reveals a distinct behavior of the hydroxyls with protons originating from the BD and MD formates, denoted $O_{br}H_{BD}$ (Figure 4b) and $O_{br}H_{MD}$ (Figure 4c). Most of the $O_{br}H_{MD}$ hydroxyls appear to be quite stable, except for some shuttling events between the surface O_{br} and the (generally deprotonated) MD formates, consistent with the results of Ref.[24]. In contrast, several protons transfer from the $O_{br}H_{BD}$ hydroxyls to second layer water molecules to form H_3O^+ ions near the interface. Compared with the BD monolayer case in Figure 3, there are more interfacial H_3O^+ ions for the mixed MD/BD interface, due to the stronger surface acidity associated with the higher FA coverage.

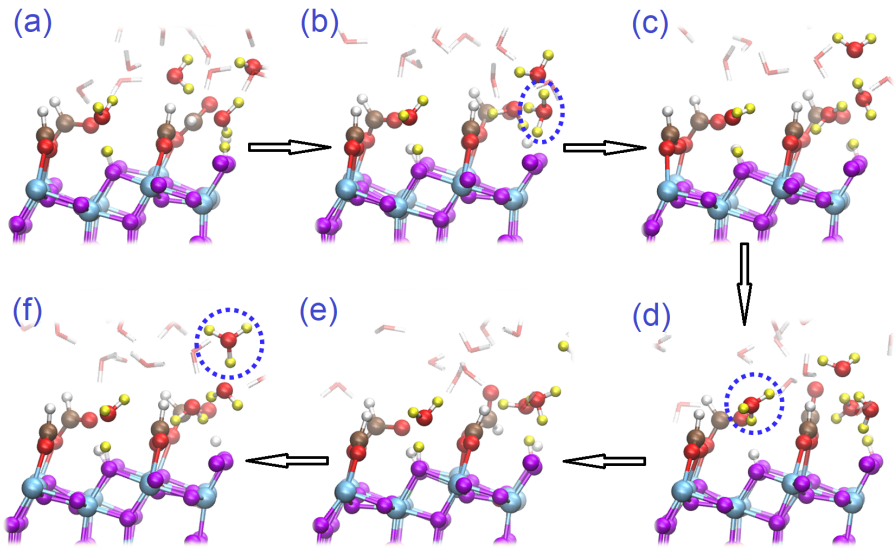

Figure 5 – (a – f) Snapshots from AIMD simulation of the **I3** interface. The snapshots, in chronological sequence indicated by the arrows, show proton transfer between surface and interfacial water resulting in H_3O^+ (blue dashed circle) formation.

A closer view of the formation of a H_3O^+ ion at interface **I3** is presented in Figure 5. In the sequence shown, proton transfer from the surface to water involves two active surface O_{br} H species and several interfacial water molecules, with a few transient transfers and exchanges occurring between different $O_{br}H$–water pairs, before one stable H_3O^+ is finally formed and leaves the interface. This can be considered as an equilibration process driven by the difference in pH between the acid monolayer covered surface and the water solvent and leads to the formation of an electrical double layer that can strongly affect the properties of the interface[23].

The process illustrated in Figure 5 provides direct evidence of the existence of H-bonds between interfacial water and surface $O_{br.}$/ $O_{br}H$ groups on the fully FA-covered A-101 surface. Further evidence is given in Figure 6, where we compare the pair correlation functions, g(r), of Ti_s-O_w, O_s-H_w, and O_s-O_w pairs for interfaces **I2** and **I3** with the analogous g(r)'s for interface **I1**. For all three interfaces, the O_s-H_w and O_s-O_w g(r)'s show peaks at ~ 1.8 and 2.8 Å, respectively, which are also the typical values of H-bonds and O-O distances in liquid water[22]. Similarly, the distributions of $O_s\widehat{H}_wO_w$ bond angles for **I2** and **I3** have peaks at 145° and 150°, respectively, only slightly smaller than the peak value of 160° for interface **I1,** where the existence of interfacial water molecules H-bonded to the surface is well established[26,35]. The presence of H-bonds at interfaces **I2** and **I3** implies that the A-101 surface covered by a FA monolayer is *not* hydrophobic. This is at variance with what was found for the rutile (110) surface, which becomes hydrophobic when covered by mixed 80% formate-20% acetate monolayers[11].

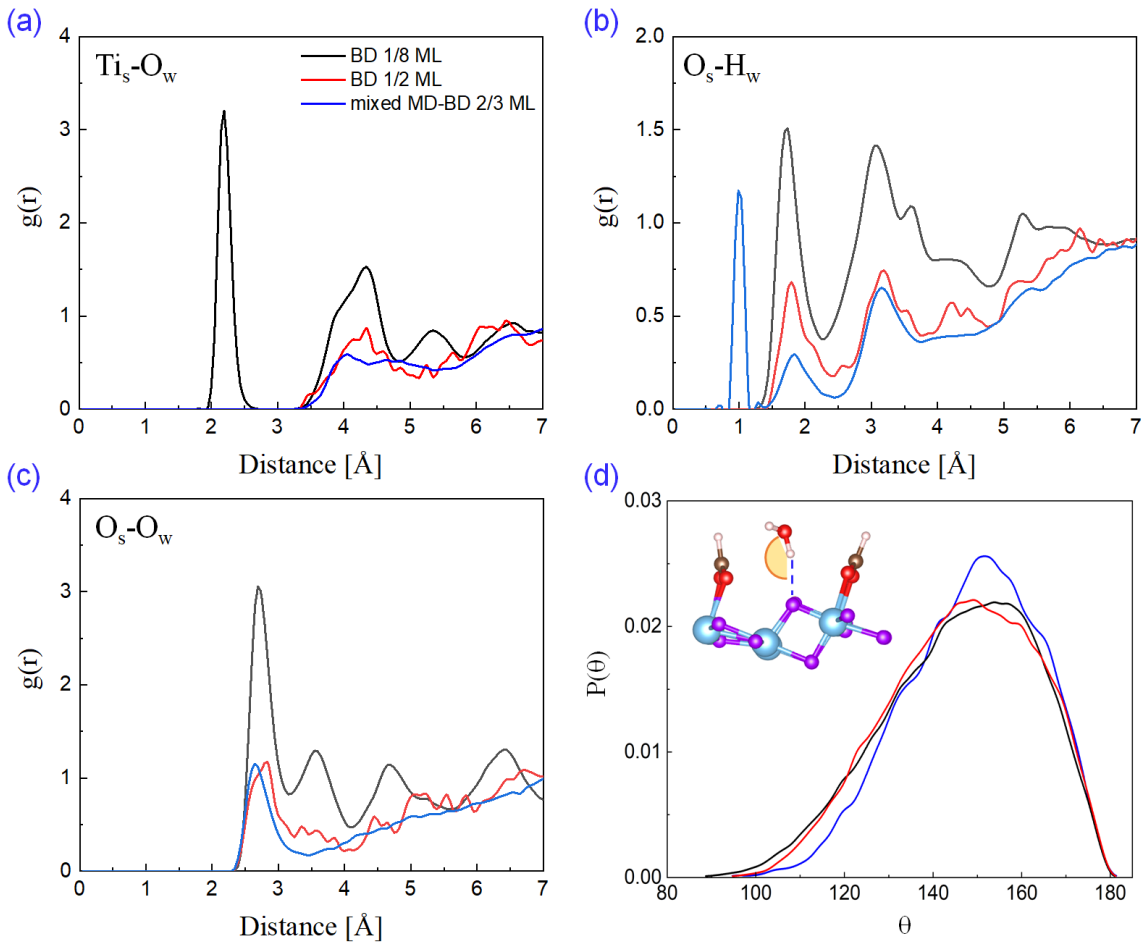

Figure 6 – Comparison of the pair correlation functions, g(r), for interfaces **I1** (BD 1/8 ML), **I2** (BD 1/2 ML) and **I3** (mixed MD-BD 2/3 ML): (a) surface Ti -water O (Ti_s -O_w), (b) surface O - water H (O_s -H_w), and (c) O_s-O_w pairs. The first peak of the Ti_s-O_w g(r) for interface **I1** originates from adsorbed water at Ti_{5c} sites; these sites are occupied by the adsorbed formates at interfaces **I2** and **I3**. The first peak of the O_s-H_w g(r) for interface **I3** is due to an exchange between an acid proton and a proton of water, as illustrated in Figure 5. Panel (d) compares the distribution of $O_s \widehat{H}_w O_w$ bond angles (sketched in the inset) for the three different interfaces.

In summary, our AIMD simulations of water / formic acid monolayer / A-101 interfaces provide direct atomic-scale insight into the process of acid proton transfer from an adsorbed carboxylate monolayer on the oxide surface to the water environment, resulting in the formation of H_3O^+ ions and an electrical double layer at the interface. Moreover, the hydration layer of the clean surface is largely but not completely suppressed when A-101 is covered by a full monolayer of bidentate or mixed monodentate/bidentate adsorbed species. This suggests that, at variance with what was found for rutile (110), the presence of an adsorbed formic acid monolayer cannot account for the hydrophobicity of anatase TiO_2 surfaces under ambient conditions.

ASSOCIATED CONTENT

Supporting Information.

The Supporting Information is available free of charge at: https://pubs.acs.org.

Computational details; Low coverage FA adsorption on A-101 in water environment: SCAN vs PBE results; Full FA monolayers on A-101 in vacuum and in water environment (SCAN results); Mixed BD/MD monolayer on A-101 in water environment: PBE results**.**

AUTHOR INFORMATION

Corresponding Authors

Annabella Selloni, Princeton University, Princeton NJ 08544; Email: aselloni@Princeton.edu

Bo Wen, Henan University, Kaifeng 475001, P. R. China; E-mail: bo.wen@henu.edu.cn

ACKNOWLEDGEMENT

We acknowledge the support of DOE BES, CSGB Division under Award DESC0007347. We also acknowledge support from the Computational Chemical Center: Chemistry in Solution and at Interfaces, funded by the DoE under Award DESC0019394. We used resources of the National Energy Research Scientific Computing Center (DoE No. DE-AC02-05cH11231) and the TIGRESS high-performance computer center at Princeton University.

References:

(1) Diebold, U. The surface science of titanium dioxide. *Surf Sci Rep* **2003,** *48* (5–8), 53.
(2) Fujishima, A.; Zhang, X.; Tryk, D. A. TiO2 photocatalysis and related surface phenomena. *Surf Sci Rep* **2008,** *63* (12), 515.
(3) Henderson, M. A. A surface science perspective on photocatalysis. *Surf Sci Rep* **2011,** *66* (6–7), 185.
(4) Chen, H.; Nanayakkara, C. E.; Grassian, V. H. Titanium Dioxide Photocatalysis in Atmospheric Chemistry. *Chemical Reviews* **2012,** *112* (11), 5919.
(5) Rajh, T.; Dimitrijevic, N. M.; Bissonnette, M.; Koritarov, T.; Konda, V. Titanium Dioxide in the Service of the Biomedical Revolution. *Chemical Reviews* **2014,** *114* (19), 10177.
(6) Wang, C.-y.; Groenzin, H.; Shultz, M. J. Comparative Study of Acetic Acid, Methanol, and Water Adsorbed on Anatase TiO2 Probed by Sum Frequency Generation Spectroscopy. *Journal of the American Chemical Society* **2005,** *127* (27), 9736.
(7) Vittadini, A.; Selloni, A.; Rotzinger, F. P.; Grätzel, M. Formic Acid Adsorption on Dry and Hydrated TiO_2 Anatase (101) Surfaces by DFT Calculations. *J Phys Chem B* **2000,** *104* (6), 1300.
(8) Galoppini, E. Linkers for anchoring sensitizers to semiconductor nanoparticles. *Coordination Chemistry Reviews* **2004,** *248* (13), 1283.
(9) Pujari, S. P.; Scheres, L.; Marcelis, A. T. M.; Zuilhof, H. Covalent Surface Modification of Oxide Surfaces. *Angewandte Chemie International Edition* **2014,** *53* (25), 6322.
(10) Nanayakkara, C. E.; Dillon, J. K.; Grassian, V. H. Surface Adsorption and Photochemistry of Gas-Phase Formic Acid on TiO2 Nanoparticles: The Role of Adsorbed Water in Surface Coordination, Adsorption Kinetics, and Rate of Photoproduct Formation. *The Journal of Physical Chemistry C* **2014,** *118* (44), 25487.
(11) Balajka, J.; Hines, M. A.; DeBenedetti, W. J. I.; Komora, M.; Pavelec, J.; Schmid, M.; Diebold, U. High-affinity adsorption leads to molecularly ordered interfaces on TiO_2 in air and solution. *Science* **2018,** *361* (6404), 786.
(12) De Angelis, F.; Di Valentin, C.; Fantacci, S.; Vittadini, A.; Selloni, A. Theoretical Studies on Anatase and Less Common TiO2 Phases: Bulk, Surfaces, and Nanomaterials. *Chemical Reviews* **2014,** *114* (19), 9708.

(13) He, Y.; Dulub, O.; Cheng, H.; Selloni, A.; Diebold, U. Evidence for the Predominance of Subsurface Defects on Reduced AnataseTiO_2(101). *Physical Review Letters* **2009,** *102* (10), 106105.
(14) Setvín, M.; Aschauer, U.; Scheiber, P.; Li, Y.-F.; Hou, W.; Schmid, M.; Selloni, A.; Diebold, U. Reaction of O_2 with Subsurface Oxygen Vacancies on TiO_2 Anatase (101). *Science* **2013,** *341* (6149), 988.
(15) DeBenedetti, W. J. I.; Skibinski, E. S.; Jing, D.; Song, A.; Hines, M. A. Atomic-Scale Understanding of Catalyst Activation: Carboxylic Acid Solutions, but Not the Acid Itself, Increase the Reactivity of Anatase (001) Faceted Nanocatalysts. *The Journal of Physical Chemistry C* **2018,** *122* (8), 4307.
(16) Zhang, H.; Zhou, P.; Ji, H.; Ma, W.; Chen, C.; Zhao, J. Enhancement of photocatalytic decarboxylation on TiO2 by water-induced change in adsorption-mode. *Applied Catalysis B: Environmental* **2018,** *224*, 376.
(17) Petrik, N. G.; Wang, Y.; Wen, B.; Wu, Y.; Ma, R.; Dahal, A.; Gao, F.; Rousseau, R.; Wang, Y.; Kimmel, G. A.et al. Conversion of Formic Acid on Single- and Nano-Crystalline Anatase TiO2(101). *The Journal of Physical Chemistry C* **2021,** *125* (14), 7686.
(18) Wang, Y.; Wen, B.; Dahal, A.; Kimmel, G. A.; Rousseau, R.; Selloni, A.; Petrik, N. G.; Dohnalek, Z. Binding of Formic Acid on Anatase TiO_2(101). *The Journal of Physical Chemistry C* **2020**, DOI:10.1021/acs.jpcc.0c06031 10.1021/acs.jpcc.0c06031.
(19) Kwon, S.; Lin, T. C.; Iglesia, E. Elementary steps and site requirements in formic acid dehydration reactions on anatase and rutile TiO_2 surfaces. *Journal of Catalysis* **2020,** *383*, 60.
(20) Sun, J.; Ruzsinszky, A.; Perdew, J. P. Strongly Constrained and Appropriately Normed Semilocal Density Functional. *Phys Rev Lett* **2015,** *115* (3), 036402.
(21) Sun, J.; Remsing, R. C.; Zhang, Y.; Sun, Z.; Ruzsinszky, A.; Peng, H.; Yang, Z.; Paul, A.; Waghmare, U.; Wu, X.et al. Accurate first-principles structures and energies of diversely bonded systems from an efficient density functional. *Nat Chem* **2016,** *8* (9), 831.
(22) Chen, M.; Ko, H. Y.; Remsing, R. C.; Calegari Andrade, M. F.; Santra, B.; Sun, Z.; Selloni, A.; Car, R.; Klein, M. L.; Perdew, J. P.et al. Ab initio theory and modeling of water. *Proc Natl Acad Sci U S A* **2017,** *114* (41), 10846.
(23) Zhang, C.; Hutter, J.; Sprik, M. Coupling of Surface Chemistry and Electric Double Layer at TiO2 Electrochemical Interfaces. *The Journal of Physical Chemistry Letters* **2019,** *10* (14), 3871.
(24) Tabacchi, G.; Fabbiani, M.; Mino, L.; Martra, G.; Fois, E. The Case of Formic Acid on Anatase TiO_2 (101): Where is the Acid Proton? *Angew Chem Int Ed Engl* **2019,** *58* (36), 12431.
(25) Perdew, J. P.; Burke, K.; Ernzerhof, M. Generalized Gradient Approximation Made Simple. *Physical Review Letters* **1996,** *77* (18), 3865.
(26) Calegari Andrade, M. F.; Ko, H. Y.; Car, R.; Selloni, A. Structure, Polarization, and Sum Frequency Generation Spectrum of Interfacial Water on Anatase TiO_2. *J Phys Chem Lett* **2018,** *9* (23), 6716.
(27) Tilocca, A.; Selloni, A. Vertical and Lateral Order in Adsorbed Water Layers on Anatase TiO_2(101). *Langmuir* **2004,** *20* (19), 8379.
(28) Tilocca, A.; Selloni, A. Structure and Reactivity of Water Layers on Defect-Free and Defective Anatase TiO_2(101) Surfaces. *J Phys Chem B* **2004,** *108* (15), 4743.

(29) Calegari Andrade, M. F.; Ko, H.-Y.; Zhang, L.; Car, R.; Selloni, A. Free energy of proton transfer at the water–TiO_2 interface from ab initio deep potential molecular dynamics. *Chemical Science* **2020**, DOI:10.1039/c9sc05116c 10.1039/c9sc05116c.

(30) Yin, W.-J.; Krack, M.; Wen, B.; Ma, S.-Y.; Liu, L.-M. CO_2 Capture and Conversion on Rutile TiO_2(110) in the Water Environment: Insight by First-Principles Calculations. *The Journal of Physical Chemistry Letters* **2015,** *6* (13), 2538.

(31) Grinter, D. C.; Nicotra, M.; Thornton, G. Acetic Acid Adsorption on Anatase TiO2(101). *The Journal of Physical Chemistry C* **2012,** *116* (21), 11643.

(32) Wen, B.; Yin, W.-J.; Selloni, A.; Liu, L.-M. Site Dependent Reactivity of Pt Single Atoms on Anatase TiO_2 (101) in Aqueous Environment. *Physical Chemistry Chemical Physics* **2020,** *22*, 10455.

(33) Liu, J.; Liu, Y.; Yang, J.; Zeng, X. C.; He, X. Directional Proton Transfer in the Reaction of the Simplest Criegee Intermediate with Water Involving the Formation of Transient H3O+. *J Phys Chem Lett* **2021,** *12* (13), 3379.

(34) Kosmulski, M. The pH dependent surface charging and points of zero charge. VI. Update. *Journal of Colloid and Interface Science* **2014,** *426*, 209.

(35) Hosseinpour, S.; Tang, F.; Wang, F.; Livingstone, R. A.; Schlegel, S. J.; Ohto, T.; Bonn, M.; Nagata, Y.; Backus, E. H. G. Chemisorbed and Physisorbed Water at the TiO2/Water Interface. *The Journal of Physical Chemistry Letters* **2017,** *8* (10), 2195.
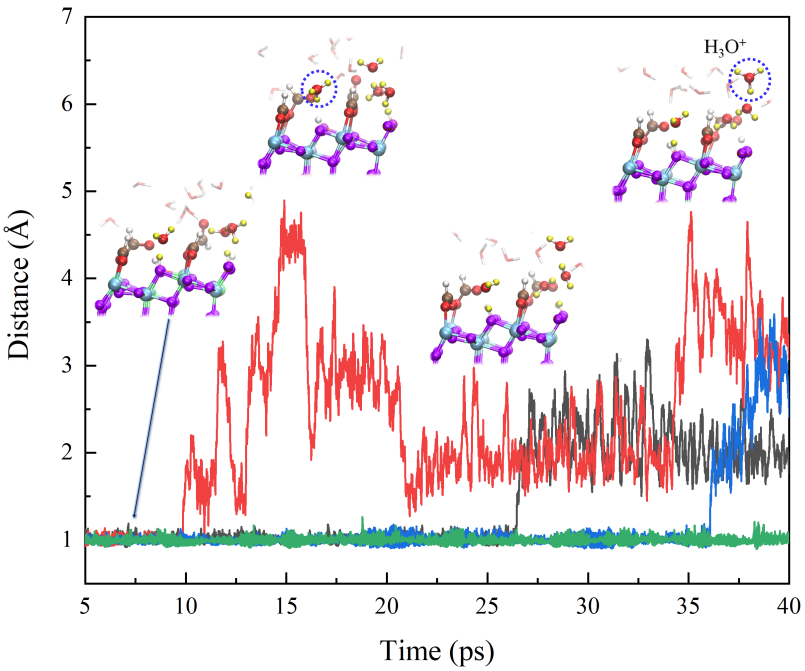
Table of Contents